# Size-induced depression of first-order transition lines and entropy-jump in extremely-layered nanocrystalline vortex matter

M.I. Dolz,[1] Y. Fasano,[2] N. R. Cejas Bolecek,[2] H. Pastoriza,[2] V. Mosser,[3] M. Li,[4] and M. Konczykowski[5]

[1]*Departamento de Física, Universidad Nacional de San Luis and CONICET, San Luis, Argentina*
[2]*Low Temperatures Division, Centro Atómico Bariloche, CNEA, Bariloche, Argentina*
[3]*Itron SAS, F-92448 Issy-les-Moulineaux, France*
[4]*Kamerlingh Onnes Laboratorium, Rijksuniversiteit Leiden, 2300 RA Leiden, The Netherlands*
[5]*Laboratoire des Solides Irradiés, Ecole Polytechnique, CNRS URA-1380, 91128 Palaiseau, France*

(Dated: June 25, 2015)

We detect the persistence of the solidification and order-disorder first-order transition lines in the phase diagram of nanocrystalline $Bi_2Sr_2CaCu_2O_8$ vortex matter down to a system size of less than hundred vortices. The temperature-location of the vortex solidification transition line is not altered by decreasing the sample size although there is a depletion of the entropy-jump at the transition with respect to macroscopic vortex matter. The solid order-disorder phase transition field moves upward on decreasing the system size due to the increase of the surface-to-volume ratio of vortices entailing a decrease on the average vortex binding energy.

PACS numbers: 74.25.Uv,74.25.Ha,74.25.Dw

Understanding size-induced structural phase transitions and size-depression of transition temperatures is crucial for the development of devices made of nanoscale building-blocks of functional materials. These blocks can be as small as nanocrystals with hundred particles or less. In the case of hard condensed matter, the physical properties and stable phases of nanocrystals strongly depend on its size and shape. For instance, the size-induced depression of characteristic temperatures and thermodynamic properties in melting,[1,2], solid-solid first-order,[3] ferromagnetic and superconducting[4] transitions has been the subject of experimental and theoretical studies in a variety of systems such as metallic nanoparticles and films, and semiconductor nanocrystals. Typically, the thermodynamic properties at phase transitions, such as entropy, enthalpy, and transition temperature, decrease when reducing the nanocrystal size.[1–4] This trend is interpreted as a result of the high proportion of particles located at the surface of the nanocrystal that have a lesser binding energy than those of the volume.

Vortex matter in high-temperature superconductors is a rich soft-condensed matter playground where relevant questions on this issue can be easily answered. The number of particles (vortices) can be tuned by varying the applied fields since the inter-vortex spacing $a \propto 1/B$.[5] Therefore nanocrystalline vortex matter can be nucleated by conveniently reducing the applied field and sample size down to tens of microns by means of lithographic engineering techniques. The binding energy of vortex matter can be selected by changing $H$ and superconducting material since it is proportional to the inter-vortex interaction energy that depends on the $a/\lambda$ ratio, with $\lambda$ the material penetration depth. In addition, the location of thermodynamic phase transitions in the density-temperature vortex phase diagram depends on the balance between three energy scales: thermal, inter-vortex and vortex-disorder interactions.[5] This balance can be tuned by temperature and choosing superconducting materials with different disorder (pinning) and vortex elastic properties. In extremely-anisotropic high-$T_c$'s this energy-competition is fostered by the softening of the vortex lattice induced by the material layerness.[5] The phase diagram of macroscopic samples is dominated by a liquid-solid first-order transition (FOT) at which the thermal energy overwhelms the binding energy. The ordered solid vortex phase presents a structural FOT to a disordered vortex glass on increasing $H$.[5] Studying the persistence or disappearance of this melting and solid-solid transitions on decreasing the number of vortices allow us to test the validity of the thermodynamic limit in FOTs.

A model high-$T_c$ material to study these issues is the layered $Bi_2Sr_2CaCu_2O_8$ compound that in its pristine form is a rather clean system. The FOT line $H_{FOT}$ in this material[6,7] separates a solid vortex phase at low fields with a liquid[8] or decoupled gas[9] of pancake vortices with reduced shear viscosity[10] in the high-temperature range. At low temperatures, the so-called second-peak, $H_{SP}$, order-disorder FOT separates the vortex solid from a glassy vortex phase at high $H$.[11] Direct imaging of vortices in pristine $Bi_2Sr_2CaCu_2O_8$ reveals the low-field vortex solid has quasi long-range positional order.[12] This phase is magnetically irreversible due to the effect of bulk pinning and surface barriers that dominate at different temperature and measuring-time ranges.[13]

The persistence of these transition lines and the evolution of their thermodynamic properties in nanocrystalline vortex matter is still open to discussion. In the case of $Bi_2Sr_2CaCu_2O_8$, Josephson-plasma-resonance data suggest that the $H_{FOT}$ transition entails a single-vortex decoupling process between stacks of pancake vortices in adjacent CuO planes.[14] This can be further tested by decreasing the system size to less than hundred vortices. This issue has not been studied probably since achieving the required experimental $B$-resolution is not straightforward. Regarding the $H_{SP}$ FOT, there is a report on its disappearance for a system with hundreds vortices.[15]

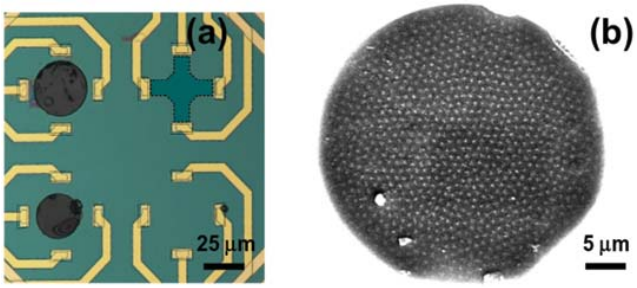


Figure 1: (a) Micron-sized $Bi_2Sr_2CaCu_2O_8$ disks mounted on the Hall sensors with $16 \times 16\,\mu m^2$ active surfaces (indicated with dotted lines). (b) Nanocrystalline vortex solid imaged by magnetic decoration at 20 Oe in a 40 $\mu$m diameter disk.

This was explained invoking bulk currents arguments in spite of their two-quadrant dc magnetization loops being dominated by surface-barrier physics.[15]

We studied the effect of confinement on the location of $H_{FOT}$ and $H_{SP}$ and on their associated thermodynamic properties by nucleating nanocrystalline vortex matter in micron-sized disks of $Bi_2Sr_2CaCu_2O_8$ single-crystals ($T_c = 90$ K). The disks, engineered by optical lithography and physical ion-milling,[16] have thicknesses of $\sim 1\,\mu$m and diameters between 20 to 50 $\mu$m. Magnetic decoration[12] experiments show the penetration of regular vortex structures as in Refs. 17,18, see Fig. 1 (b). Vortices are observed at distances smaller than 1 $\mu$m from the edge indicating no degradation of the sample edge as a result of the preparation method.

The local magnetization of the disks, $H_s$, was measured using 2D electron gas Hall sensors with $16 \times 16\,\mu m^2$ active surfaces. Figure 1 (a) shows two of the studied disks glued onto the sensors with Apiezon N grease to improve thermal contact. A local coil generates an ac field $H_{ac}$ parallel to the dc one, with amplitudes ranging $1 - 3$ Oe rms and frequencies between 1 to 200 Hz. dc and ac local magnetic measurements were performed using the same set-up as a function of temperature, magnetic field, and frequency. In the ac measurements we simultaneously acquire the in- and out-of-phase components of the fundamental and the third-harmonics of the Hall voltage using a digital-signal-processing lock-in (EG&G 7265). The in-phase component of the first-harmonic signal, $B'$, is used to calculate the transmittivity of the vortex system $T' = [B'(T) - B'(T \ll T_c)]/[B'(T > T_c) - B'(T \ll T_c)]$.[19] This magnitude is more sensitive to discontinuities in the local induction than direct measurements of the static $B$. The modulus of the normalized third harmonic signal $|\,T_{h3}\,|$[19] is non-negligible when the magnetic response becomes non-linear. Our ac data have a resolution of 5 mG, one order of magnitude better than dc measurements.

Figure 2 contrasts the magnetic response of the smallest measured 20 $\mu$m disk with that of the macroscopic sample from which the disks were engineered. For the disks the detection of the $B$-jump at $H_{FOT}$ is elusive in dc loops, see top panel of Fig. 2 (a). Performing ac

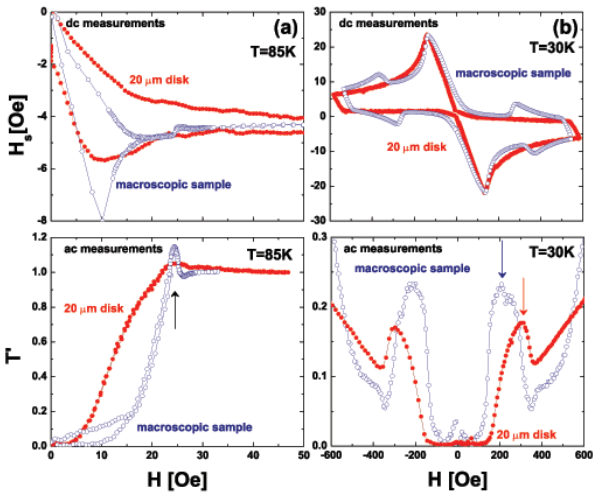


Figure 2: Magnetic response of nanocrystalline and macroscopic $Bi_2Sr_2CaCu_2O_8$ vortex matter. (a) The $H_{FOT}$ transition is detected as a jump in the dc sample field (top panel) and as a peak in the ac transmittivity (bottom panel). (b) The order-disorder $H_{SP}$ field is taken at the onset of the increase in critical current, see arrows.

$T'(H)$ measurements allows determining $H_{FOT}$ in the disks from the field-location of the paramagnetic peak entailed at this FOT, see arrow in Fig. 2 (a). The paramagnetic peaks are located at the same field for the macroscopic sample and the disks. The nearly-vanishing remanent magnetization and the two-quadrant locus of the dc loops of the disks indicate a larger influence of surface barriers for vortex flux entry/exit. Performing ac magnetometry is then imperative to have access to the faster decaying bulk currents emerging from the surface-barrier background[13] and therefore to properly track FOT lines in nanocrystalline vortex matter.

Figure 3 shows $T'(T)$ and $|\,T_{h3}(T)\,|$ data for the 20 $\mu$m diameter disk for low number of vortices, $76 < n_v < 304$. The paramagnetic peak fingerprinting the $H_{FOT}$ is clearly visible for a nanocrystal of only 76 vortices (5 Oe). This peak shifts to lower temperatures on increasing $H$ and echoes in the $|\,T_{h3}(T)\,|$ signal, indicating the high-resolution of our ac measurements. Similar behavior in $T'(T)$ and $|\,T_{h3}(T)\,|$ are also observed for the 30, 40, and 50 $\mu$m-diameter disks. These results are summarized in the vortex phase diagram of Fig. 4. The $H_{FOT}$ transition line is obtained from tracking the paramagnetic peak in the temperature-field plane. For $T < 75$ K no paramagnetic peak is detected, presumably due to a masking effect produced by enhanced surface barriers in small samples. In the case of the disks, the $H_{FOT}$ line merges that of the macroscopic reference sample.

Therefore, the $H_{FOT}$ transition persists and no melting-point depression is observed even for a nanocrystal with less than hundred vortices. Ordinary melting is the result of thermal breaking of the inter-particle bonds. In nanocrystals the average binding energy,

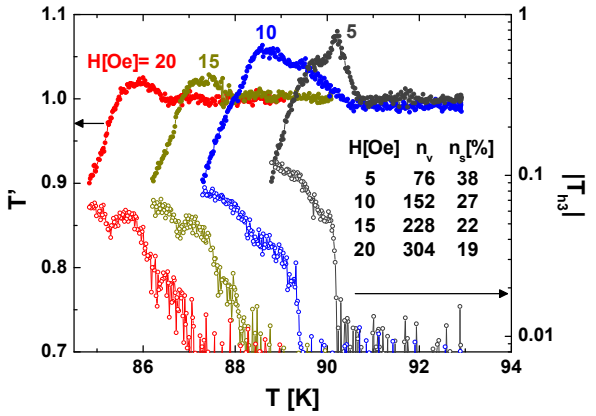


Figure 3: Temperature-evolution of the transmittivity and third-harmonic for the 20 $\mu$m diameter disk. For each measurement $H$ we show the number of vortices nucleated in the sample, $n_{\rm v}$, and the surface-to-volume vortex ratio, $n_{\rm s}$.

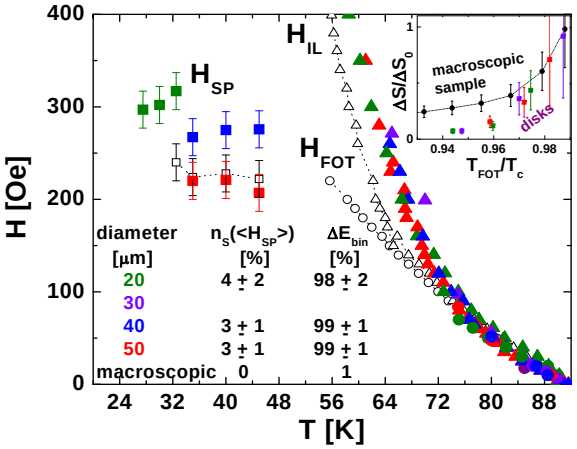


Figure 4: Phase diagram of nanocrystalline and macroscopic[16] $Bi_2Sr_2CaCu_2O_8$ vortex matter indicating the surface-to-volume vortex ratio for the average $H_{\rm SP}$, $n_{\rm s}(<H_{\rm SP}>)$, and the nanocrystal-to-macroscopic bindig energy ratio, $\Delta E_{\rm bin}$. Insert: Normalized entropy-jump at $H_{\rm FOT}$.

$<E_{\rm bin}>$, is smaller since the considerable fraction of particles located at the surface, $n_{\rm s}$, has a lesser binding energy. The ratio between the nanocrystalline-to-macroscopic $<E_{\rm bin}>$ can be obtained in a rough estimation as $\Delta E_{\rm bin} = (0.5 n_{\rm s}) + (1 - n_{\rm s})$, the first term coming from considering that the binding energy of vortices of the outer shell is reduced to half the value for vortices at the interior of the sample, considered in the second term. For instance, for the smallest measured nanocrystal $n_{\rm s} = 38\,\%$ and $\Delta E_{\rm bin} \sim 80\,\%$, a decrease of $<E_{\rm bin}>$ that in hard condensed matter should be enough in order to produce a noticeable melting-point depression.[2] *Since for nanocrystalline $Bi_2Sr_2CaCu_2O_8$ vortex matter this is not observed, the symmetry broken at $H_{\rm FOT}$ should be other than the in-plane inter-vortex bonds.* There is evidence that in $Bi_2Sr_2CaCu_2O_8$ the $H_{\rm FOT}$ transition occurs concomitantly with a c-axis decoupling between pancake vortices of adjacent CuO planes.[14] For the smallest system we studied the number of pancake vortices is larger than 50.000. Considering this, our results suggest that the broken symmetry on cooling at $H_{\rm FOT}$ is the establishment of the c-axis superconducting phase coherence produced by the coupling of pancake vortices in the whole sample thickness, rather than an improvement of the in-plane structural order of vortex matter exclusively. Indeed, in-plane disordered vortex structures are nucleated in irradiated samples that still present a $H_{\rm FOT}$ transition.[20]

Other thermodynamic properties rather than $T_{\rm FOT}$ are however affected by decreasing the sample size. The insert to Fig. 4 shows the evolution of the normalized entropy-jump, $\Delta S/\Delta S_0$, at the liquid-solid transition for nanocrystalline and macroscopic $Bi_2Sr_2CaCu_2O_8$ vortex matter. The entropy-jump at the transition, $\Delta S$, is shown normalized by the $\Delta S_0$ value extrapolated at zero field. The $\Delta S$ versus reduced temperature $T_{FOT}/T_{\rm c}$ data were obtained from applying the Clausius-Clapeyron relation, $\Delta S \propto (\Delta B/B_{\rm FOT}) dH_{\rm FOT}/dT$,[16] with $\Delta B$ the enthalpy-jump. In the case of the disks the enthalpy was estimated from $T'(T)$ data considering that at the transition $T' = 1 + (2\Delta B)/(\pi H_{\rm ac})$[16]. The data for the disks with 50 to 20 $\mu$m diameter are packed in a single trend of $\Delta S/\Delta S_0$ lying below the macroscopic sample data.

Since the $T_{\rm FOT}$ does not vary with the system size in the range studied, this decrease in $\Delta S$ comes from a decrease on the enthalpy entailed in the transition for nanocrystalline vortex systems. Therefore, irrespective of the system size, vortex matter undergoes a solidification transition at the same $T_{\rm FOT}$ entailing the same type of symmetry breaking. However, assuming that the entropy of the liquid is independent of the system size, the solid nanocrystalline vortex matter has a larger entropy than macroscopic crystals. In previous works we reported that there is an increase of the density of topological defects in nanocrystalline vortex matter with respect to the macroscopic case.[18] Therefore the sample-size-induced enthalpy-jump decrease in the $H_{\rm FOT}$ transition is in agreement with a worsening of the positional in-plane structural order induced by confinement effects.

In order to better understand these findings, theoretical work on the sample-size dependence of the entropy-jump at the FOT and the electromagnetic-to-Josephson interactions ratio is required. Any attempt of quantitative explanation of this evolution should include a realistic model on the evolution of the binding energy on decreasing the system size for extremely-layered vortex matter. Another issue that must be considered is that probably the $\Delta S$ reduction on decreasing the system size is connected to disorder introduced by sample fabrication being more relevant on increasing the surface-to-volume ratio. Disorder affects the $\Delta S$ curve producing a downward shift at low $T_{\rm FOT}/T_{\rm c}$ as recently reported.[17]

We also study the effect of decreasing the vortex number on the solid order-disorder $H_{\rm SP}$ transition. Figure 2 (b) compares dc and ac results: While the dc loops do not show evidence of $H_{\rm SP}$ for the 20 $\mu$m disk, local maximum and minimum in the ac data are evident. These features come from the increase in critical current entailed in the $H_{\rm SP}$ transition, detected by applying the ac technique more sensitive to bulk current contributions. Therefore the previously reported absence of the $H_{\rm SP}$ transition for micron-sized $Bi_2Sr_2CaCu_2O_8$ samples[15] comes from technical limitations of dc magnetic techniques for which surface currents play a determining role in screening.[13]

In order to quantify the effect of decreasing the number of vortices on the solid order-disorder transition we tracked this line considering the onset of the effect associating $H_{\rm SP}$ to the local maximum in $T'(H)$. Figure 4 shows a remarkable result: On decreasing the sample size $H_{\rm SP}$ monotonically moves up in $H$ increasing the field-stability of the ordered low-field vortex-solid phase. The $H_{\rm SP}$ line, as any structural solid-to-solid FOT, entails a small discontinuity in the binding energy that is smaller for the disordered phase, the high-field vortex-glass. At a given field, when decreasing the sample size $n_{\rm s}$ is enhanced and then the $< E_{\rm bin} >$, and accordingly $\Delta E_{\rm bin}$, are smaller than for a larger nanocrystal. The fraction of surface-to-volume vortices at the average value of the almost temperature-independent $H_{\rm SP}$, $n_{\rm s}(< H_{\rm SP} >)$, is of the order of $4 \pm 2\,\%$ for all the studied micron-sized disks (see Fig. 4). Considering this information, and our rough estimation for the decrease in the $< E_{\rm bin} >$ of vortex nanocrystals, $\Delta E_{\rm bin} \sim (98 \pm 2)\,\%$ at the average $H_{\rm SP}$, independently of the sample size. The order-disorder transition condition is that at $H_{\rm SP}$ the elastic energy of the vortex system, proportional to its binding energy, is balanced by the interaction energy of vortices with the disorder introduced by pinning.[5] Since no dramatic changes in the pinning energy are introduced by our method of decreasing the sample size as observed in the dc loops of Fig. 2,[21] in order to reach this energy-balance condition when decreasing the sample size, $H$ has to be increased such to attain the same interaction energy $\propto \Delta E_{\rm bin}$.

The non-thermodynamic line at which magnetic response becomes irreversible, $H_{\rm IL}$, is also affected by confinement. For nanocrystalline vortex matter this line is located at higher fields than for the macroscopic case, see Fig. 4. This might have origin in the different aspect-ratio of the samples, and in their probably dissimilar surface roughness. In the high-temperature range the $H_{\rm IL}$ lines for nanocrystalline and macroscopic vortex matter merge into a single bunch of data with the $H_{\rm FOT}$ line. At high fields, the onset of $\mid T_{\rm h3} \mid$ develops before the paramagnetic peak on cooling, see Fig. 3, indicating the existence of a narrow non-linear vortex region spanning at $H > H_{\rm FOT}$.[22] This phase-region might have origin on a residual effect of pinning[23], or Bean-Livingston barriers[24] on the liquid phase. This phenomenology was already detected in macroscopic samples, although spanning a larger phase region than in vortex nanocrystals.[16]

In conclusion, the liquid-to-solid FOT remains robust and persists at the same location even when decreasing the system size to less than hundred vortices. This supports the scenario of the FOT line being a single-vortex decoupling transition[14] that depends, at best, on the density of the surrounding vortex matter. The entropy-jump entailed in the transition decreases for nanocrystalline vortex matter in agreement with direct-imaging experiments revealing a worsening of the positional order with respect to the macroscopic case.[18] The solid order-disorder FOT at $H_{\rm SP}$ also persists on decreasing the system size down to 20 $\mu$m contrary to what has been reported.[15] The $H_{\rm SP}$ moves upward on reducing the sample size such as the average binding energy of the nanocrystal, and thus its interaction energy, remains roughly the same. The identification of these FOTs increases in difficulty when decreasing the sample size due to the predominance of surface-barrier-related currents and therefore applying ac magnetometry is mandatory in order to improve the sensitivity to bulk currents.


[1] C.J. Coombes, J. Phys. F: Metal Phys. **2**, 441 (1972).
[2] A. N. Goldstein, C. M. Echer, and A. P. Alivisatos, Science **256**, 1425 (1992).
[3] S. H. Tolbert and A. P. Alivisatos, Science **265**, 373 (1994).
[4] G.Guisbiers and L.Buchaillot, Phys. Lett. A **374**, 305(2009).
[5] G. Blatter *et al.*, Rev. Mod. Phys. **66**, 1125 (1994).
[6] H. Pastoriza *et al.*, Phys. Rev. Lett. **72**, 2951 (1994).
[7] E. Zeldov *et al.*, Nature **375**, 373 (1995).
[8] D. R. Nelson, Phys. Rev. Lett. **60**, 1973 (1988).
[9] L. I. Glazman and A. E. Koshelev,Phys. Rev. B **43**, 2835(1991).
[10] H. Pastoriza and P. H. Kes, Phys. Rev. Lett. **75**, 3525(1995).
[11] N. Avraham *et al.*, Nature **411**, 451 (2001).
[12] Y. Fasano, J. Herbsommer and F. de la Cruz, Phys. Stat. Sol. B **215**, 563 (1999).
[13] N. Chikumoto *et al.*, Phys. Rev . Lett. **69** 1260 (1992).
[14] S. Colson *et al.*, Phys. Rev. Lett. **90**, 137002 (2003).
[15] Y. M. Wang *et al.*, Physica C **341**, 1109 (2000).
[16] M. I. Dolz *et al.*, Phy. Rev. B **90**, 144507 (2014).
[17] M. I. Dolz *et al.*,J. Phys. Conf. Series, **568** 022010 (2014).
[18] N. R. Cejas Bolecek *et al.*, J. Low Temp. Phys. **179**, 35 (2015).
[19] J. Gilchrist and M. Konczykowski, Phys. C **212**, 43 (1993).
[20] M. Menghini *et al.*, Phys. Rev. Lett. **90**, 147001 (2003).
[21] N. R. Cejas Bolecek *et al.*, unpublished.
[22] M. V. Indenbom *et al.*, J. Low Temp. Phys. **105**, 1117 (1996).
[23] V. M. Vinokur *et al.*, Z. Eksp. Teo. Fiz. **100**, 1104 (1991).
[24] D. Fuchs *et al.*, Nature (London) **391**, 373 (1998).